Turbidimetric Behavior of Colloidal Particles in Beer Before Filtration Process

Elisa I. Benítez, Nancy M. J. Martínez Amezaga, Gladis L. Sosa, Nélida M. Peruchena & Jorge E. Lozano

Food and Bioprocess Technology
An International Journal

ISSN 1935-5130

Food Bioprocess Technol
DOI 10.1007/s11947-012-0905-7

Springer

Food Bioprocess Technol
DOI 10.1007/s11947-012-0905-7

ORIGINAL PAPER

Turbidimetric Behavior of Colloidal Particles in Beer Before Filtration Process

Elisa I. Benítez · Nancy M. J. Martínez Amezaga · Gladis L. Sosa · Nélida M. Peruchena · Jorge E. Lozano

Received: 1 September 2011 / Accepted: 27 May 2012

Abstract The effect of colloidal particles and yeast on turbidity of Pilsen beer before the filtration process was studied in this work. The colloidal particles are mainly composed of polysaccharides, representing 96.89 %, in second place proteins with a concentration close to 2 %, and polyphenols less than 0.3 %. There is also a very low concentration of yeast (<0.25 %). The presence of different types of particles in the sample caused multimodal histogram in the particle size distribution and four distinct zones were identified: (1) very small individual particles ($\overline{D} = 0.06\mu$m), (2) yeast ($\overline{D} = 3\mu$m), (3) colloidal aggregates ($\overline{D} = 17\mu$m), and (4) a zone with a high dispersion of size, with two $\overline{D}$ values (101 and 200 μm). Particles size counts well correlate with both the scanning electron microscopy (SEM) digital image analysis, and the turbidity determination. The fractal dimension (D_f) of the aggregates was determined by analyzing the SEM images with the Variogram method, obtaining D_f>2.4 values. Those values are typical of aggregates formed by rapid flocculation or diffusion limited aggregation. Results of this study support the formulation of a model valid for the prediction of colloidal particles concentration in beer.

Keywords Beer characterization · Colloidal particles · Filtration process

Introduction

The beer after fermentation shows a significant turbidity due to the presence of yeast and the cellular tissue comminuted during the malt processing. To produce a clear beverage, the colloidal particles must be removed in order to get a good visual appearance and a pleasant taste of the final product (Fleet and Siebert 2005; Siebert 2006). A rest period of several days to remove by settling the most of yeast and cellular tissues is usually demanded (Bamforth 2003). Nevertheless, after this period some colloid particles still remain in suspension causing a significant turbidity. Therefore, beer filtration is required (Atkinson 2005; Fillaudeau et al. 2007; Bamforth 2009). Finally, the beer is usually treated with insoluble absorbents to remove haze precursors (Briggs et al. 2004).

Several tests for determination of the appropriate doses of filter aid (turbidity and filterability) are available. Although these determinations are necessary, they do not suffice to control the flux of filtrate. The filtration process reduces the turbidity to commercial levels, but in some cases, the reduction of flux causes the replacement of a filter and a complete discharge of the cake and filter aid renewal. This procedure is often much more expensive than predicted by the previous tests. For this reason, the determination of the influence of yeast and cellular tissue on the turbidity could be important to understand the behavior of the flow of filtrate.

E. I. Benítez (✉) · N. M. J. M. Amezaga · G. L. Sosa
Laboratorio de Química Teórica y Experimental (QuiTEx),
Facultad Regional Resistencia,
Universidad Tecnológica Nacional,
French 414,
3500 Resistencia, Chaco, Argentina
e-mail: ebenitez@frre.utn.edu.ar

N. M. Peruchena
Lab. Estructura Molecular y Propiedades. Departamento de Química, FACENA, Universidad Nacional del Nordeste,
Av. Libertad 5460,
3400 Corrientes, Argentina

J. E. Lozano
PLAPIQUI (UNS-CONICET),
Camino La Carrindanga Km.7,
8000 Bahía Blanca, Argentina

Published online: 19 June 2012

The turbidity of dispersion depends on the characteristics of its particles: concentration, size, and relative refractive index (McClements 2005). The average diameter ($\overline{D}$) and the nephelometric turbidity (τ) are easy to measure and are widely used parameters to describe the characteristic particle size and turbidity of commercial beverages. The expression of Eq. 1 has been useful to describe the turbidimetric behavior of colloidal particles of apple juice (Benítez et al. 2007b), which is an adaptation of equation proposed by Dobbins and Jizmagian (1966):

$$\tau_n = \frac{3}{2}\frac{C}{\rho_m}\frac{Q_{av}}{\overline{D}} \quad (1)$$

where ρ_m is the density of the continuous phase, C is the particle concentration, and Q_{av} is the nephelometric average scattering efficiency of the polydisperse, irregular particles with average diameter $\overline{D}$. Scattering efficiency depends on the particle size, the refractive indices of the particle and the continuous phase, and the wavelength of the incident light.

As cellular tissues and yeast have distinct concentrations and distinct sizes, the contributions to turbidity will be also different. For this reason, on one hand it is mentioned like colloidal particles of cellular tissue and on the other hand like yeast, although for its size it is considered as colloid particles.

To establish the influence of the yeast and colloidal particles on turbidity it would be necessary to understand its aggregation mechanism. A methodology based on the determination of fractal dimension (D_f) from juice particles images obtained by scanning electron microscopy (SEM) has shown to be useful to explain the behavior of colloidal aggregates (Benítez et al. 2010) and could be used in this case.

One of the most influential factors on turbidity is pH, since it could modify the interactions between particles. In yeast suspensions with an initial concentration of cell on the order of 10^3 CFU/mL, and pH 4–5 turbidity was modified in more than 100 NTU (Narong and James 2006), with an average size of 8 μm. In another study (Chang and Chang 2002), the change was of 30 NTU with 6.4 μm particles and a concentration of 10^6 CFU/mL. However, methods used to obtain the colloidal suspension in each case were different. In the present study, colloidal beer particles are mostly composed of polysaccharides: largely dextrins, glucans, and arabinoxylans (Sadosky et al. 2002). These particles are not electrically charged and therefore they would not being modified by the pH. In this case, due to the coexistence of different chemicals species, it would be appropriate to determine the pH influence on turbidity.

Through these determinations an average Q_{av} for both colloidal particles and yeast cells could be estimated, in order to contribute to a better understanding the phenomenon of colloidal haze in beer.

Materials and Methods

Beer Preparation

The mashing was carried out in a 40L stainless steel container. The mashing procedure started by mixing 7.5 kg of milled malted barley (Cargill Malt Division, Argentina) with deionized water at 62±2 °C for 90 min. The water/malt ratio was 4:1. Finally, the wort was boiled for 1 h with the addition of more water to complete a final volume of 40 L and hop. This bitter wort was then settled down for 30 min before it was cooled down to 12 °C. The lager yeast (Saflager S-23, Fermentis, France) was pitched at the rate of 6 g viable cells/l. The fermentation was carried out at 12± 2 °C for a period of 15 days, followed by a maturation of 7 days and a cold rest at 3±2 °C for another 2 days.

pH Effect

The pH of beer was varied from 3 to 6 using dilute acid or alkali acid as appropriate. The addition of solution of 1 N HCl (Anedra, Buenos Aires) was used to acidified and a 1 N NaOH solution (Anedra, Buenos Aires) was used to elevate the pH over 4.5. Initial beer pH was 4.5. Each sample was prepared in triplicate.

Preparation of Samples with Different Yeast and Cellular Tissue Concentration

Initial particle concentration, C_0 (in grams per liter), of each sample was determined as follows. A certain volume (20 mL) of beer was micro-filtered through a 0.45-μm cellulosic membrane (E04WP04700, MSI, Westboro, MA), such that all the beer particles were retained in the filter paper, which was previously weighed. Finally, the filter with the particles was vacuum dried at 55–60 °C overnight, and then weighed.

An arrangement of 36 samples with variable amount of colloidal particles and yeast concentration was used. The concentration of the colloidal particles (in grams per liter) was obtained by dilution at 0, 20, 40, 60, 80, and 100 % of C_0 microfiltered beer, free of colloidal particles, and was used as solvent.

The initial concentration of yeast was determined from the calibration curve between the recount in Neubauer-counting chamber N_y (number of yeast per milliter) and the concentration (C_y, in grams per liter) obtained by weighting and suspension of the same in microfiltered beer (Fig. 6). The growth of yeast in the solution was of 0, 0.2, 0.5, 1.0, 1.5, and 2.0 g/L. This variation of yeast concentration was used since it reproduces the final conditions of the fermentation process. Samples were prepared in triplicate.

Sample Preparation for Scanning Electron Microscopy

To obtain SEM images of the primary particles and aggregates, diluted samples of beer (1 mL of beer in 100 mL of water) were fixed with 2.5 % glutaraldehyde in phosphate buffer pH 7.2. Droplets of the same in the fixed material were put in glass coverslips with polylysine film for 1 h. Polylysine (ε-poly-L-lysine (EPL)) is a polymeric substance that shows a net attractive electrostatic potential (Thomas et al. 1996). Therefore, aggregates are attracted to the EPL. Then the coverslip was washed with the same buffer, dehydrated with 25, 50, 75, 80 %, and three times with 100 % solutions of acetone. Finally, the coverslips was desiccated with a critic point drier (Polaron E3000 CPD, EEUU) with acetone and CO_2 as intermediate fluids. The samples were gold sputtered with an automatic sputter coater (Sputter Coater, Pelco 91000) and analyzed by SEM (LEO, EVO 40, Cambridge, UK) at 20 kV accelerating voltage.

Analysis of Particles and Aggregates

Twenty different SEM images of the particles and the aggregates were analyzed with the Variogram method for the determination of D_f. The Variogram method is based on the calculation of the variance of V of the brightness level distribution of a sample surface image and was well described in the bibliography (Bonetto and Ladaga 1998; Bianchi and Bonetto 2001; Bonetto et al. 2002):

$$V = \Delta\left\langle \Sigma \mathrm{zi}^2 \right\rangle \approx s^{2H} \tag{2}$$

where Δzi is the bright level difference between two different positions in a digital image for a step i of length s, measured in pixels or microns, and the in brackets denote the expectation value (Bonetto and Ladaga 1998). The value of H is obtained from the slope of $log(V)$ vs $log(s)$, as shown in Fig. 5. This value is related to the fractal dimension as follows:

$$D_f = 3 - H \tag{3}$$

The software FERImage (Bianchi and Bonetto 2001) was used for this purpose and is freely available at http://www.cindeca.org.ar/programas.

Physicochemical Determinations

Turbidity was measured using the Oakton T-100 Turbidimeter (Oakton Instr., IL, USA) at 25 °C. The measure was made at 30 min after the inoculation of the samples with the yeast solution.

Particles diameter and the size distribution were measured using a laser-scattering particle size distribution analyzer (LA-950, Horiba Ltd., France) at 25 °C. The data were obtained and analyzed using the program Horiba LA-950 for Windows Ver. 2.0. The Particle size calculation was based on the Mie-Scattering theory. Results obtained are the average of five determinations per sample. Density of the liquid medium (ρ_m) was determined by pycnometry.

The initial concentration of colloidal particles after fermentation, C_0 (in grams per liter), was determined as follows. A certain volume (≈20 mL) of beer was micro-filtered through a 0.45-μm cellulosic membrane (E04WP04700, MSI, Westborough, MA), such that all the colloidal particles were retained in the filter paper, which was previously weighed. The filter with the particles was vacuum dried at 55–60 °C overnight and weighed. Determinations were made at least in triplicate.

Composition of filter-retained material was calculated using the concentration of components in beer before and after filtration. Cell concentration of yeast was determined with a Neubauer-counting chamber. Protein content (P) was determined using the Bradford method (1976). Total polyphenol content (TPP) was determined with the Folin–Ciocalteu method (Singleton et al. 1999) and total polysaccharides with the phenol-sulfuric method of Segarra et al. (1995). All determinations were made in triplicate at least.

Statistical Analysis

Data points were presented as the mean of the measured values. The data were subjected to an analysis of variance and the Turkey test at the 0.05 level of significance (Infostat 2002).

Results and Discussion

Particle Size Distribution and Fractal Dimension Determination

The initial concentration of colloidal particles after fermentation was 5.15±0.01 g/L Compositional analysis of material retained by the filter resulted to be polysaccharides, representing 96.89 %; proteins (2 %); and polyphenols (<0.3 %). It was also detected a very low concentration of yeast cells (≤0.25 %) whose effect on beer turbidity must be considered. Traces (≤0.5 %) of other non-identifiable compounds were also determined (Table 1).

Microstructure of beer colloidal particles could be observed in the SEM images of Fig. 1. Values obtained by image analysis were correlated with particle size distribution data. Figure 1 shows a colloidal aggregate, whose fractal structure allows clearly visualize the small particles composing the aggregate. It also could be observed a large number of small isolated particles surrounding the colloidal aggregate. On the other hand, in Fig. 2, a large aggregate of

Table 1 Initial composition of the colloidal particles

	g/L
C_0	5.15±0.01
TPS	4.99±0.02
P	0.101±0.003
TPP	0.015±0.002
C_y	0.013±0.004
UI	0.03±0.02

Concentration (N=3) data are mean values±standard deviation

UI un-identifiable, *P* protein content, *TPP* total polyphenol content, *TPS* total polysaccharides

yeast, which also have a fractal structure (fractile cluster) and a colloidal particle close to a yeast cell, can be observed (Fig. 2a).

The different size species, present in beer haze shown in Fig. 2, generated a multimodal histogram (Fig. 3). The multimodal particle size distribution histogram shows an extent from 0.03 to 300 μm. The highest diameter value and cumulative volume percentage of each peak are also indicated in Fig. 3. Four different zones were identified: (1) very small individual particles ($\overline{D} = 0.06 \pm 0.01\mu$m), (2) yeast ($\overline{D} = 3 \pm 0.6\mu$m), (3) colloidal aggregates ($\overline{D} = 17 \pm 2\mu$m), and (4) a zone with a high dispersion of size, with two $\overline{D}$ values (101±14 and 200±7 μm) attributed to yeast aggregates. A great volumetric percentage of yeast and aggregates of yeast was observed. However, after converting particle size from a volume basis to a number basis, results indicated that the smaller particles represent more than 99 % of beer turbidity. The average diameters of the different species involved are listed in the Table 2, as well as the fractal dimension and the cumulative volume percentage values.

The existence of two $\overline{D}$ values for the yeast aggregates could be an effect of the large extension of them, the particles may be bi- or even trimodal. While obtained histograms show to be basically monomodal for individual yeast, individual particles and colloidal aggregates, yeast aggregates exhibits a bimodal behavior. Scattering intensity dependence on particle's cross-sectional area could explain these results (Siebert 2009).

Figure 4 shows the graphics used for the determination of the fractal dimension of colloidal aggregates. H value, obtained from the slope of the curve (Fig. 4) resulted H= 1.049±0.05 for the case of the aggregate shown in Fig. 2. From Eq. 4, D_f=2.48±0.05 was calculated. It was preceded in the same way for yeast aggregates and individual particles.

The aggregation of colloidal particles leads to the formation of highly branched aggregates, with a fractal structure formed by the mechanism of diffusion-limited aggregation (DLA), wherein a diffusing particle "hits and sticks" to the cluster in the same position where it arrived (Benítez et al. 2010). The presence of an energy barrier between particles slows down the collision frequency, resulting in slow flocculation or reaction limited aggregation (RLA). In general, for DLA yield structures with D_f=2.5 flocs grow by adding

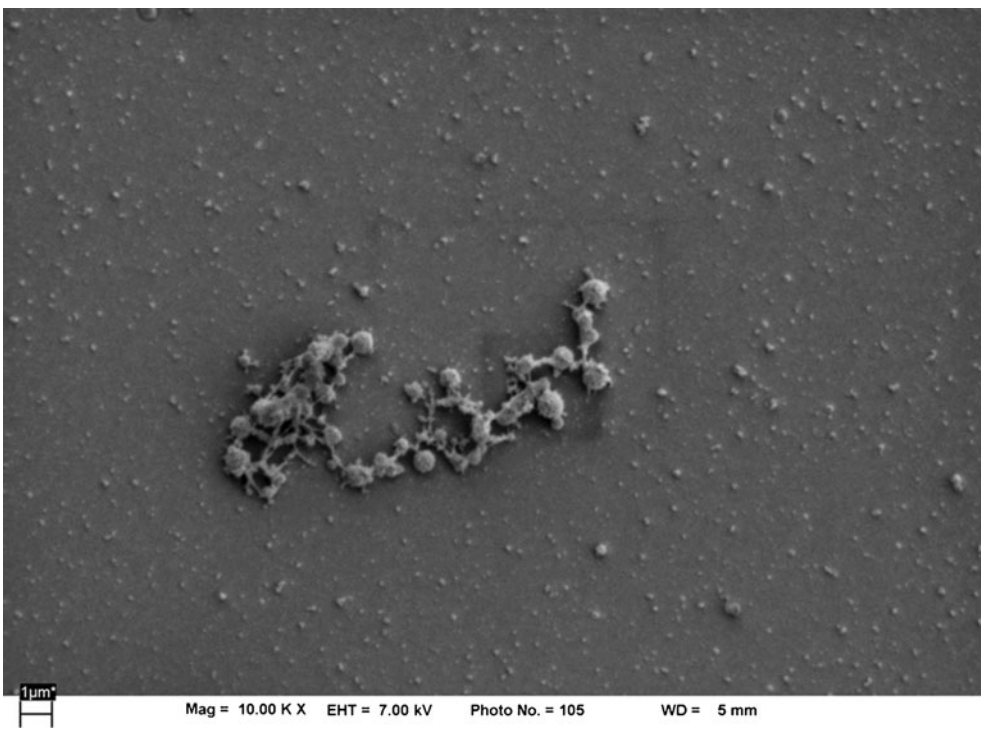

Fig. 1 SEM image of primary particles and a colloidal particles aggregate, obtained after dilution of beer. Magnification, ×10,000. Scale, 1 μm=70 pixels

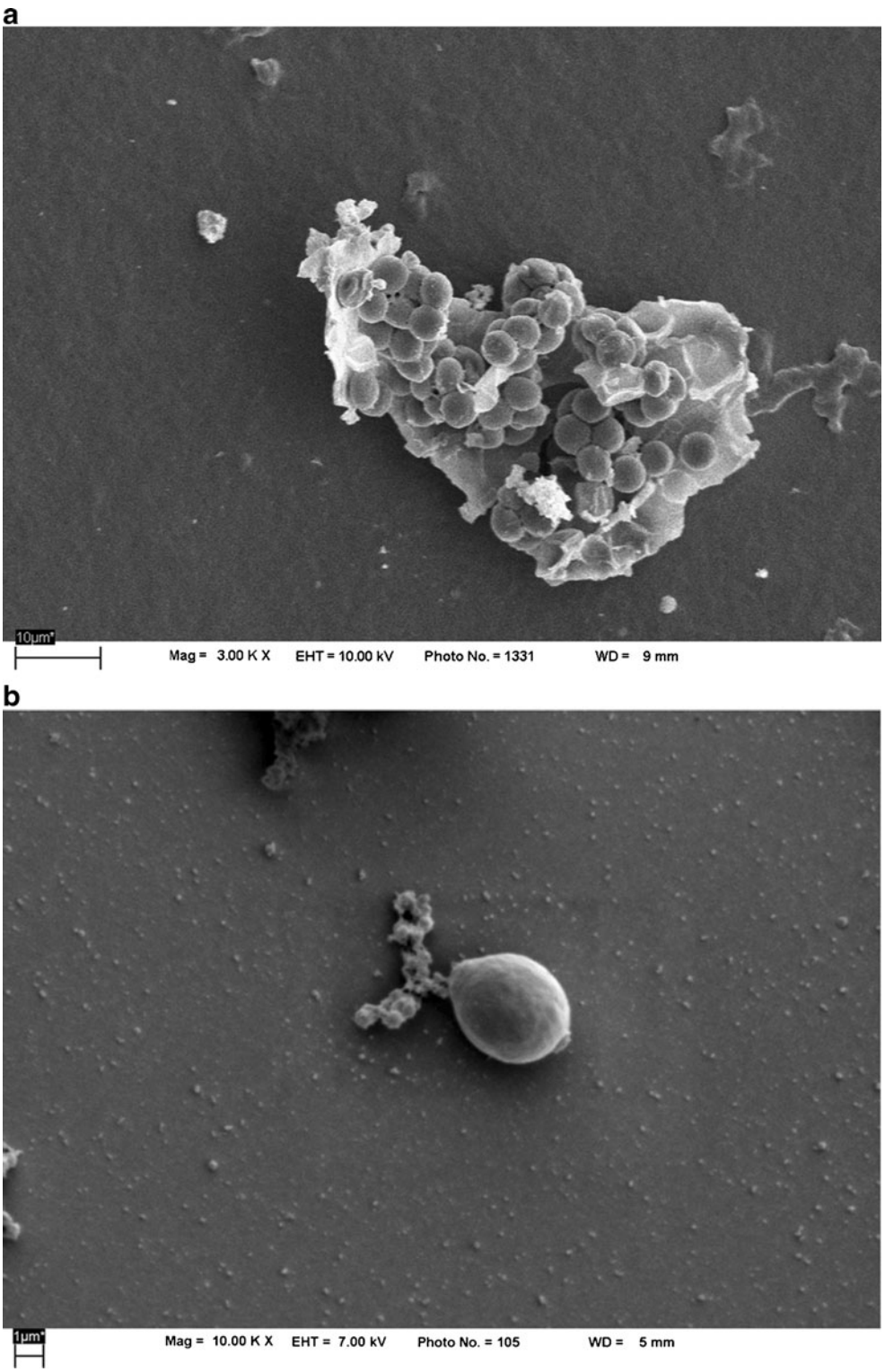

Fig. 2 SEM images of **a** a yeast with a colloidal particle aggregate (magnification, ×10,000; scale, 1 μm=70 pixels) and **b** a colloidal aggregate of yeast (magnification, ×3000; scale, 10 μm=101 pixels), obtained after dilution of beer

one particle at a time, but this value drops to D_f=1.75 if cluster–cluster aggregation predominates. On the other hand, RLA gives values of D_f=2.0–2.2. (Russel et al. 1989; Berli et al. 1999). The average fractal dimension value obtained by statistical analysis of the SEM images for every single case resulted D_f>2.4, indicating rapid flocculation or DLA by incorporation of individual particles, and not by aggregate-aggregate interaction (a D_f value close to 1.75 would be obtained in that case) (Russel et al. 1989). The colloidal particles with sizes <0.1 μm are generally very

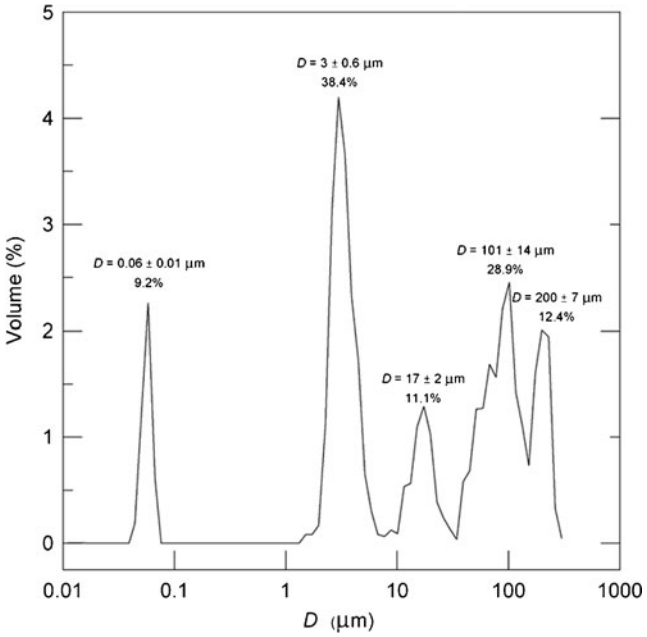

Fig. 3 Particle size distribution of colloidal suspension of beer

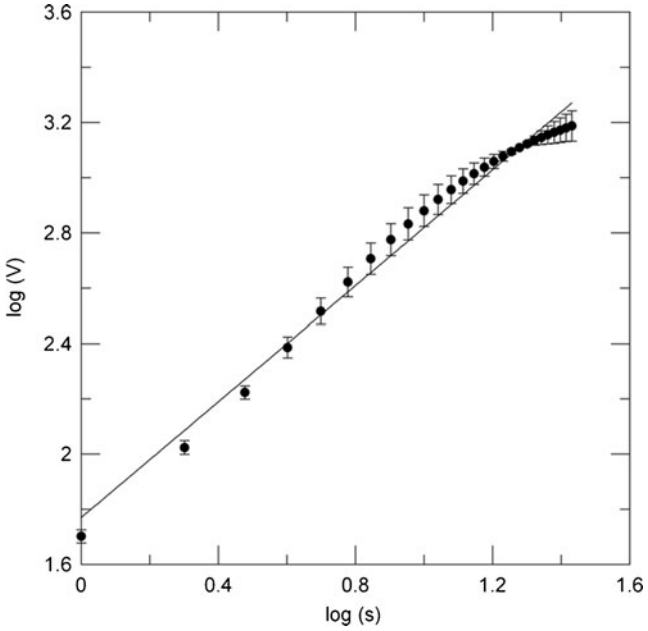

Fig. 4 Correlation between the logarithmic plot of the variance (V) of the brightness level distribution of a sample surface image and the length (s), measured in pixels and obtained with the Variogram method applied to the aggregate of Fig. 1. *Vertical bars* represent the standard deviation in each value

unstable and trends to quickly associate to form aggregates. Once formed, these primary aggregates are typically stable for more extended periods of time (Lencki and Riedl 1999). The existence of very small colloidal particles could be related with the formation of the post-packing haze described in the bibliography (Bamforth 2009; Siebert 2009), attributed to the failing of filters to retain the smaller particles, which agglomerate into larger particles after certain time of bottling.

The aggregation of yeast respond to another factor: After a certain elapsed time, due to deficiency of nutrients and the action the environmental factors, yeast cells begin to agglomerate and precipitate. The yeast in adverse condition produces specific surface glycoproteins capable of directly binding mannoproteins of adjacent cells. Both, cell surface charge and hydrophobicity, are also implicated in this mechanism (Pretorius 2000).

Nevertheless, the formation of yeast aggregates after fermentation is the result of the incorporation of individual yeast cells and not by the interaction of aggregates, as D_f value suggests.

pH Effect

The studied colloidal suspension presented a great pH stability in the range of pH analyzed (pH=3–6). An oscillating variation around an average turbidity value ($\bar{\tau} = 85 \pm 5$ NTU) was observed. No significant statistical differences between values ($p<0.05$) were determined. It was assumed that both (1) the prevailing number of small particles and (2) the effect of the liquid media surrounding yeast cells reinforce colloid stability, and therefore, consolidate beer turbidity. This negligible variation in turbidity was also observed in cloudy apple juice (Benítez et al. 2007a), attributed in this case to a high energy of hydration of particles, preventing the contact between them. In the case of study, the same behavior was observed, indicating no interaction among beer yeast aggregates, and a gradual one-to-one incorporation of particles to aggregates with time. Moreover, the small amount of observable yeast cells, as compared with the large number of small

Table 2 Physicochemical properties of colloidal particles and yeast cells

	$\overline{D}$ (μm)	Volumen (%)	D_f	Q_{av} (NTU m)
Individual particles	0.06±0.01	9.2	2.43±0.04	0.35
Individual cell of yeast	3±0.6	38.4	2.47±0.03	59.84
Aggregate of particles	17±2	11.1	2.48±0.05	98.54
Aggregates of yeast 1	101±14	28.9	2.54±0.04	2014.65
Aggregates of yeast 2	200±7	12.4	2.54±0.04	3989.40

$\overline{D}$ (N=5) and D_f (N=3) data are mean values±standard deviation

particles of different origin, was considered to stabilize the colloidal system preventing interaction among aggregates.

Influence of the Colloidal Particles and Yeast Cells on Turbidity

In order to compare both colloidal particles and yeast cells contribution to turbidity, they must be expressed in the same units. Therefore, the concentration of yeast aggregates was correlated with the cell recount in counting chamber. A linear fit of data with a good correlation (R^2=0.975) was obtained (Fig. 5):

$$N_y = 2.29 \times 10^6 \cdot C_y \quad (4)$$

where N_y represents the number of yeast per milliliter and C_y represents the concentration of yeast expressed in grams per liter. This determination allowed expressing the turbidity as a function of the recount of yeast in the sample.

In accordance with theoretical Eq. 1, beer turbidity was found to be directly proportional to concentration (Fig. 6). Accordingly, the experimental data were fitted to:

$$\tau = b \cdot C_y \quad (5)$$

where b is known as the specific turbidity (Dickinson 1994).

Owing to the coexistence of yeast and other colloidal particles, a modification of Eq. 5 having into consideration the effect of the colloidal particles resulted in:

$$\tau = \tau_p + b\, C_y \quad (6)$$

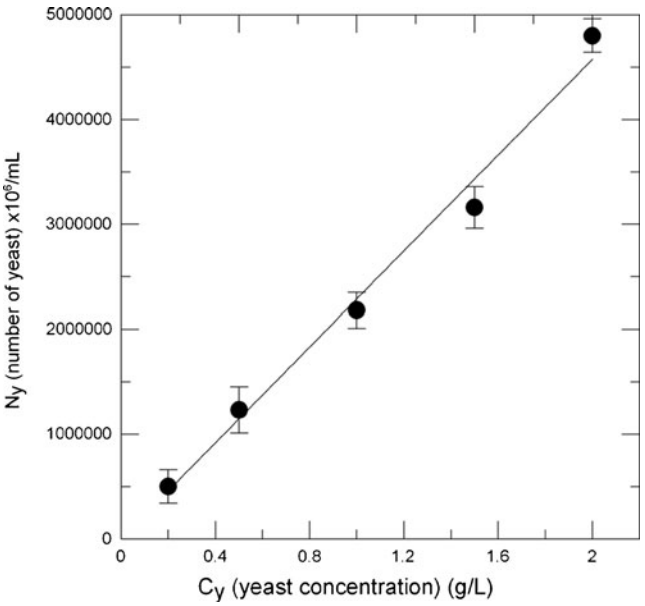

Fig. 5 Correlation between concentrations of yeast expressed as number of yeast per milliliter and grams per liter fitted with Eq. 5. *Vertical bars* represent the standard deviation in each value

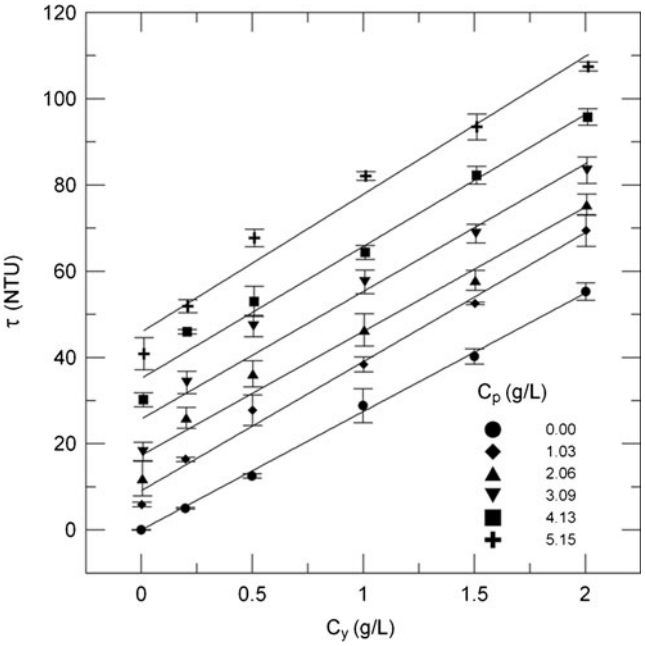

Fig. 6 Correlation between turbidity and concentration of yeast (C_y) at different concentration of colloidal particles (C_p), fitted with Eq. 7. *Vertical bars* represent the standard deviation in each value

Being τ_p the coordinate at the origin of the curve. τ_p and b values, as well as the correlation parameter R^2, were listed in Table 3. The component τ_p followed a linear relationship with C_p, according to the function (R^2=0.997):

$$\tau_p = 8.6\, C_p \quad (7)$$

where C_p is the concentration of colloidal particles in grams per liter.

Slopes resulted not significantly different (p<0.05). Therefore, averaging slopes values (Eq. 8) were obtained:

$$\tau = 29.8\, C_y + 8.6\, C_p \quad (8)$$

Where C_y and C_p coefficients represent the values of turbidity in absence of yeast and colloidal particles, respectively, and correspond to the specific turbidity.

Table 3 Equation 7 fitting parameters for different colloidal particles concentration (C_P)

C_p (g/L)	τ_p (NTU)	d (NTU L/g)	R^2
0.00	29.4±1 a	0.0	0.998
1.03	29.9±2 a	9.1	0.989
2.06	28.8±3 a	17.3	0.975
3.09	29.6±2 a	25.7	0.957
4.13	30.4±2 a	34.5	0.967
5.15	30±2 a	45.9	0.974

τ_p (N=3) data are mean values±standard deviation. Means in same column with equal lowercase letters are not significantly different (p<0.05)

To equal concentration of yeast and particles, yeast turbidity resulted 3.4 times higher than the turbidity due to colloidal particles. This phenomenon can be attributed to differences in volume and shows a large coherence all through the determinations. Q_{av} values, for each involved turbidity species, was also calculated. Using the average $\overline{D}$ values, the solvent density obtained by pycnometry (ρ_m= 1.008±0.001 g/mL) and the specific turbidity, the nephelometric average scattering efficiency resulted:

$$Q_{av} = \frac{2}{3} \cdot b \cdot \rho_m \cdot \overline{D} \quad (9)$$

The values of Q_{av} are listed in Table 2, where can be observed that Q_{av} for small colloidal particles is very low as compared with that of the yeast cells, which are of the same order of magnitude than the colloidal aggregate. The individual yeast and the colloidal aggregates of particles contribute to the 49.5 % of the total volume of species in the suspension (Table 2), and in a minor degree to the yeast aggregates. Therefore, even though Q_{av} values for yeast aggregates are high, the small number of them limited their influence on the turbidity. These results indicate that the turbidity determination could be used to quantify an overall concentration of colloidal particles, with the help of the yeast cell counting.

The reduction in beer filtration flux is mainly due to polysaccharides concentration (Sadosky et al. 2002). The effect of beer polysaccharides on turbidity was negligible, compared with the significant contribution of yeast cells to haze formation (Table 1).

Results also suggested that the only determination of turbidity is not enough to check and control the filtrate flux in the beer industry, and more studies need to be done.

Conclusions

This work confirmed and quantified the formation of fractal aggregates by obtaining a fractal dimension value which is consistent with the DLA mechanism. The result contributes to the understanding of the structure, aggregation, and stability of colloid particles in beer. Furthermore, this study helps to identify the main significant variables in beer turbidity and could provide information about the possible contribution to the flux of filtrate. However, the great amount of small particles are masked by the large size of the yeast cells, and permitted to conclude that turbidity, being a factor to take into consideration, is not conclusive regarding the reduction of the flux of filtrate. Moreover, yeast cells count should be considered to obtain a more accurate idea of beer turbidity composition. Further studies are required to quantitatively determine the effect of colloidal particles and yeast on the flux of filtrate and, finally, correlate flux and turbidity. These studies are now in progress.

Acknowledgments The authors acknowledge Facultad Regional Resistencia-UTN, PLAPIQUI-UNS y CONICET for financial support.

References

Atkinson, S. (2005). Beer clarification. *Membrane Technology, 2005*, 8–9.

Bamforth, C. (2003). Refining matters—downstream processing. In: *Beer: Tap into the Art and Science of Brewing* (pp. 159–170). New York: Oxford University Press

Bamforth, C. (2009). Colloidal stability of beer. In: *Beer: a quality perspective* (pp. 111–161). New York: Academic Press

Benítez, E., Genovese, D., & Lozano, J. (2007a). Effect of pH and ionic strength on apple juice turbidity: application of the extended DLVO theory. *Food Hydrocolloids, 21*, 100–109.

Benítez, E., Genovese, D., & Lozano, J. (2007b). Scattering efficiency of a cloudy apple juice: effect of particles characteristics and serum composition. *Food Research International, 40*, 915–922.

Benítez, E., Lozano, J., & Genovese, D. (2010). Fractal dimension and mechanism of aggregation of apple juice particles. *Food Science and Technology International, 16*, 179–186.

Berli, C., Deiber, J., & Añón, M. (1999). Heat-induced phenomena in soy protein suspensions. Rheometric data and theoretical interpretation. *Journal of Agricultural and Food Chemistry, 47*, 893–900.

Bianchi, F., & Bonetto, R. (2001). FERImage: an interactive program for fractal dimension, d_{per} and d_{min} calculation. *Scanning, 23*, 193–197.

Bonetto, R., & Ladaga, J. (1998). The variogram method for characterization of scanning electron microscopy images. *Scanning, 20*, 457–463.

Bonetto, R., Forlerer, E., & Ladaga, J. (2002). Texture characterization of digital images which have a periodicity or quasi-periodicity. *Measurement Science and Technology, 13*, 1458–1466.

Bradford, M. (1976). A rapid and sensitive method for the quantitation of microgram quantities of protein utilizing the principle of protein-dye binding. *Analytical Biochemistry, 72*, 248–554.

Briggs, D., Boulton, C., Brookes, P., & Stevens, R. (2004). Beer maturation and treatments. In: *Brewing science and practice* (pp. 543-587). Cambridge: Woodhead Publishing Limited

Chang, Y., & Chang, P. (2002). The role of hydration force on the stability of suspension of *Saccharomyces cerevisiae*—application of the extended DLVO theory. *Colloids and Surfaces A: Physicochemical and Engineering Aspects, 211*, 67–77.

Dickinson, E. (1994). Colloidal aspects of beverages. *Food Chemistry, 51*, 343–347.

Dobbins, R., & Jizmagian, G. (1966). Optical scattering cross sections for polydispersions of dielectric spheres. *Journal of the Optical Society of America, 56*, 1345–1350.

Fillaudeau, L., Boissier, B., Moreau, A., Blanpain-avet, P., Ermolaev, S., Jitariouk, N., & Gourdon, A. (2007). Investigation of rotating and vibrating filtration for clarification of rough beer. *Journal of Food Engineering, 80*, 206–217.

Fleet, C., & Siebert, K. (2005). Effect of illumination intensity on visual perception of turbidity. *Food Quality and Preference, 16*, 536–544.

Infostat (2002). *InfoStat versión 1.1*. Grupo Infostat, FCA, Universidad Nacional de Córdoba, Argentina

Lencki, R., & Riedl, K. (1999). Effect of fractal flocculation behavior on fouling layer resistance during apple juice microfiltration. *Food Research International, 32*, 279–288.

McClements, D. (2005). *Food emulsions: principles, practice, and techniques*. London: CRC Press.

Narong, O., & James, A. (2006). Effect of pH on the ζ-potential and turbidity of yeast suspensions. *Colloids and Surfaces A: Physicochemical and Engineering Aspects, 274*, 130–137.

Pretorius, I. (2000). Tailoring wine yeast for the new millennium: novel approaches to the ancient art of winemaking. *Yeast, 16*, 675–729.

Russel, W., Saville, D., & Schowalter, W. (1989). *Colloidal dispersions*. Cambridge: Cambridge University Press.

Sadosky, P., Schwarz, P., & Horsely, R. (2002). Effect of arabinoxylans, β-glucan, and dextrins on the viscosity and membrane filterability of a beer model solution. *Journal of the American Society of Brewing Chemists, 60*, 153–162.

Segarra, I., Lao, E., López-Tamames, E., & De la Torre-Boronat, M. (1995). Spectrophotometric methods for the analysis of polysaccharides levels in winemaking products. *American Journal of Enology and Viticulture, 46*, 564–570.

Siebert, K. (2006). Haze formation in beverages. *Food Science and Technology, 39*, 987–994.

Siebert, K. (2009). Haze in beverages. *Advances in Food and Nutrition Research, 57*, 53–86.

Singleton, V., Orthofer, R., & Lamuela-Raventos, R. (1999). Analysis of total phenols and other oxidation substrates and antioxidants by means of Folin Ciocalteau reagent. *Methods in Enzymology, 299*, 152–178.

Thomas, N., Coakley, W., & Winters, C. (1996). Contact formation in polylysine-mediated membrane-glass interaction. *Colloids and Surfaces B, 6*, 139–147.